Globally Optimal Synthesis of Heat Exchanger Networks. Part III: Non-Isothermal Mixing in Minimal and Non-Minimal Networks

Chenglin Chang[1], Zuwei Liao[2], André L. H. Costa[3] and Miguel J. Bagajewicz[4]*

[1]*Zhejiang Provincial Key Laboratory of Advanced Chemical Engineering Manufacture Technology, College of Chemical and Biological Engineering, Zhejiang University, Hangzhou 310027, P. R. China.*

[2]*State Key Laboratory of Chemical Engineering, College of Chemical and Biological Engineering, Zhejiang University, Hangzhou 310027, P. R. China.*

[3]*Rio de Janeiro State University (UERJ), Rua São Francisco Xavier, 524, Maracanã, CEP 20550-900, Rio de Janeiro, RJ, Brazil Rio de Janeiro*

[4]*School of Chemical, Biological and Materials Engineering, University of Oklahoma, Norman, Oklahoma, 73019, USA.*

CORRESPONDING AUTHOR: *Zuwei Liao. E-mail address: liaozw@zju.edu.cn

Keywords: Heat exchanger networks; Non-isothermal mixing; Global optimum search algorithm.

ABSTRACT

In this work, the enumeration algorithms presented in parts I and II for the globally optimal synthesis of heat exchanger networks are extended to consider non-isothermal mixing. The previous models are modified by adding non-isothermal mixing constraints and new models are constructed to target the bounds of the energy consumption and the binding exchanger minimum approximation temperature. These new models are solved using algorithms that involve solving the solution of systems of equations instead of mathematical programming. We also present two alternatives for optimizing each enumerated structure, namely, the use of a global solver, or the use of a golden search with simple resolution of non-isothermal mixing model for fixed energy consumption. The non-isothermal mixing model is reformulated as a convex model, either solved using nonlinear programming or a programming-free methodology, i.e. solving Karush-Kuhn-Tucker equations. A global optimum search algorithm is developed and examples are tested comparing the proposed strategies.

Keywords: Heat exchanger networks; Non-isothermal mixing; Global optimum search algorithm.

1. Introduction

The synthesis of heat exchanger networks (HEN) is a well-known research topic in Process Systems Engineering. Numerous design technologies and methods have been developed and published with extensive applications to industrial practices, as described in several review articles[1-3] and some research publications,[4-6] to name a few. Of all these previous works on HEN synthesis, the approach that gains large dominance is the one where superstructure-based models are formulated as mixed integer nonlinear models (MINLM), which can be solved using mixed integer nonlinear programming (MINLP) procedures,[7-9] many times using decompositions,[10-12] or using stochastic-based methods (metaheuristics-based methods), such as genetic algorithms (GA),[13-15] simulated algorithm (SA),[16,17] particle swarm optimization (PSO),[18,19] hybridization between different algorithms,[20-22] etc. However, we do not elaborate further with a literature review of these alternative methods and focus on the uses of the MINLP procedures. Most of the time, the MINLP procedures do not guarantee global optimality or fail to be sucsessfuly solved through commercial global solvers such as BARON, ANTIGONE, etc. In turn, the stochastic/metaheuristics-based methods do not guarantee optimality, much less global optimality, and in general need specialized parameter tuning for a good computational performance.

The two most popular superstructures used in previous literature are, respectively, the one developed by Floudas et al.[23] which was further generalized by Kim and Bagajewicz,[24] and the stage-wise one established by Yee and Grossmann[25] which was used or/and extended by Huang et al,[26] Mistry and Misener,[27] Pavão et al.,[28] Beck and

Hofmann,[29] Nair and Karimi,[30] etc. All these previous works were reviewed in the parts I nd II of this research.[31,32] The attempts to globally solve these above superstructure-based models by using commercial global solvers exhibited computational difficulties especially in medium- and large-size case studies, even without non-isothermal mixing. Some successful attempts were implemented via a non-commercial procedure namely Rysia.[33,34]

Departing from the exclusive use of MINLP procedures in the parts I and II of this research,[31,32] we relied on a novel solution procedure based on exhaustive enumeration as well as the smart enumeration of structures, aided by low demanding mathematical programming procedures. The smart enumeration we refer to is Option 1 in parts I and II, where a lower bound of the problem is used to generate structures one by one, with a stopping criteria consisting of determining that the lower bound is higher than the incumbent best result. The important point is that global optimality is obtained for all different sizes of problems, even large ones with both enumeration approaches.

In this research, we extend the previous algorithms presented in our parts I and II to further consider non-isothermal mixing for HEN synthesis. Similar to our previous algorithms, we exhaustively enumerate HEN structures (stream matches) by using a combination of mixed integer linear models (MILMs) solved using mixed integer linear programming (MILP) procedure (see our part I and II) to obtain the candidate structures. For each structure, the network cost is optimized for the energy consumption (hot utility demand) and the binding exchanger minimum approximation temperature (EMAT) by using a Golden Search strategy and the direct computation of exchanger areas. Small-and medium- size examples, the most common in industrial practices, were solved in competitive time. In the case of large-scale problems (15-39 streams), global optimality was also achieved, but the computational time increased. Two issues are worth noticing for large-scale problems:

(1) We know these problems had been near-globally solved by using stochastic or metaheuristic procedures,[35-37] although tuning of parameters is likely to be needed;

(2) We also know that without good initial points global solvers (BARON and ANTIGONE) many times fail[38-40] while other solving procedures like Rysia[33,34] have memory and time problems. Thus, having a tool for global optimization albeit time consuming is an advance. Future work will be aimed to reduce the computational time.

In our current extension of the enumeration algorithm, we use two approaches to optimize each enumerated structure:

- First Approach: A global solver is used for each generated structure without using a Golden Search, as it was done in Parts I and II (we name it Strategy 1).
- Second Approach: Use a Golden Search, optimizing the flowrate capacities of the split streams for each splitting instance. This optimization could be done by using an nonlinear model (NLM) and we name it Strategy 2, or by solving the Karush-Kuhn-Tucker (KKT) equations and we name it Strategy 3.

Strategy 3 relies entirely on the algorithms that solve systems of equations for each candidate structure. We point out in the case of exhaustive enumeration, the candidate structures are obtained using a mixed integer linear optimization model, which can be solved with other algorithms based on graph theory. This is not the case of Option 1, where the lower bound can't be easily solved algorithmically. Thus, the potential exists to solve this synthesis problem globally without using mathematical programming.

The rest of this paper is structured as follows. First, three global optimization strategies are presented. Then, we describe some properties of non-isothermal mixing for HENs and prove that the NLM for optimizing the flowrate capacities of the split streams is convex. Following, the formulations of several new models and algorithms are given. Next, the proposed Global Search Algorithm is presented. Finally, nineteen examples are tested for illustration purposes. Conclusions follow.

2. Global Optimization Strategies

Three different strategies that rely on enumerating structures by running *PLB* or *PSTR* models (see our part I) for exhaustive enumeration are presented below. As discussed in our parts I and II, global optimality is achieved in both cases (*PLB* and *PSTR*).

- Strategy 1: For each fixed structure being enumerated, initialize a global solver (we used BARON) with the solution results of the enumeration procedure (*PLB* or *PSTR*), and solve the resulting nonlinear programming (NLP) model (see Supplemental Material-Part A) considering non-isothermal mixing to global optimality. This strategy avoids the use of the Golden Search. BARON is known to exhibit problems in the case wherein the integer variables are not fixed (i.e.

the structure is not fixed) and/or when poor initial values are given. However, we find that, after fixing the integers, solving the resulting NLP using BARON with fixed integer variables works well in small- and medium-scale examples but fails in large-scale ones.

- Strategy 2: Proceed with the Golden Search algorithms developed in our parts I and II, for each value of the energy consumption and the binding EMAT, solve a NLM to minimize the area cost only for the heat exchangers that are involved in stream splits. These are isolated structures consisting of a few heat exchangers, a result of limiting the total number of heat exchangers.
- Strategy 3: Proceed with the Golden Search algorithms developed in our parts I and II, and solve the system of equations based on the KKT conditions corresponding to the aforementioned NLM.

In the next section, we prove that the NLM corresponding to Strategy 2 and 3 is a convex problem. Then, the equations of the KKT conditions for Strategy 3 are presented (Supplemental Material-Part C).

It is worth mentioning that Strategy 3, aside from the generation of structures, can be implemented without any other tool than a solver of systems of equations, with no mathematical programming involved. Moreover, knowing that structures can be generated algorithmically by exploiting graph theory properties, Strategy 3 can potentially be the first mathematical programming-free procedure for globally optimal HEN synthesis.

3. Convex Model for Flow Optimization in Stream Splits

Consider a hot stream and a cold stream involved in splits, as depicted in Figure 1.

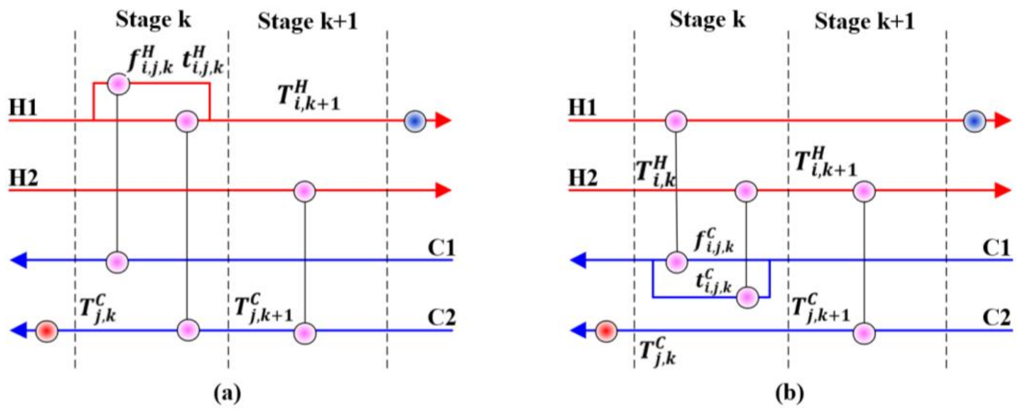

Figure 1. Stream splits and nomenclature: (a) Hot stream split; (b) Cold stream split.

Binary parameters $Y^H_{i,k}$ and $Y^C_{j,k}$ are defined to respectively denote whether hot stream i and cold stream j are split or not at stage k. For a structure, the values of the binary variables $z_{i,j,k}$, zhu_j and zcu_i that represent the existence of heat exchangers are given, and they are written as $\hat{z}_{i,j,k}$, $\hat{z}hu_j$ and $\hat{z}cu_i$. Then, the values of $Y^H_{i,k}$ and $Y^C_{j,k}$ are assigned as follows.

$$Y^H_{i,k} = \begin{cases} 1 & \sum_{j \in CP} \hat{z}_{i,j,k} > 1 \\ 0 & \text{Otherwise} \end{cases} \qquad \forall i \in HP, k \in ST \tag{1}$$

$$Y^C_{j,k} = \begin{cases} 1 & \sum_{i \in HP} \hat{z}_{i,j,k} > 1 \\ 0 & \text{Otherwise} \end{cases} \qquad \forall j \in CP, k \in ST \tag{2}$$

As demonstrated in part I, the heat loads ($\hat{q}_{i,j,k}$, $\hat{q}hu_j$ and $\hat{q}cu_i$) for a minimum structure (MSTR) network (minimal network) are unique once energy consumption ($\hat{E}$) is fixed. The same can be said in the case of non-MSTR network (non-minimal network) with the fixed hot utility (energy) consumption and fixed binding EMAT (see our part II). For minimal and non-minimal HENs with a fixed energy consumption and a fixed binding EMAT, the heat loads of heat exchangers are fixed and the stream temperatures at stages are also fixed, and each stage can be solved independently of the others. Hence, of those, only the ones that have split require a nonlinear model to minimize area cost.

We recall that the stream temperatures at each stage upon mixing $\hat{T}^H_{i,k}$ and $\hat{T}^C_{j,k}$ are fixed parameters because of the overall energy balances for each stage. This is depicted in Figure 2, which illustrates instances of MSTR and non-MSTR networks with the fixed energy consumption and the fixed binding EMAT respectively.

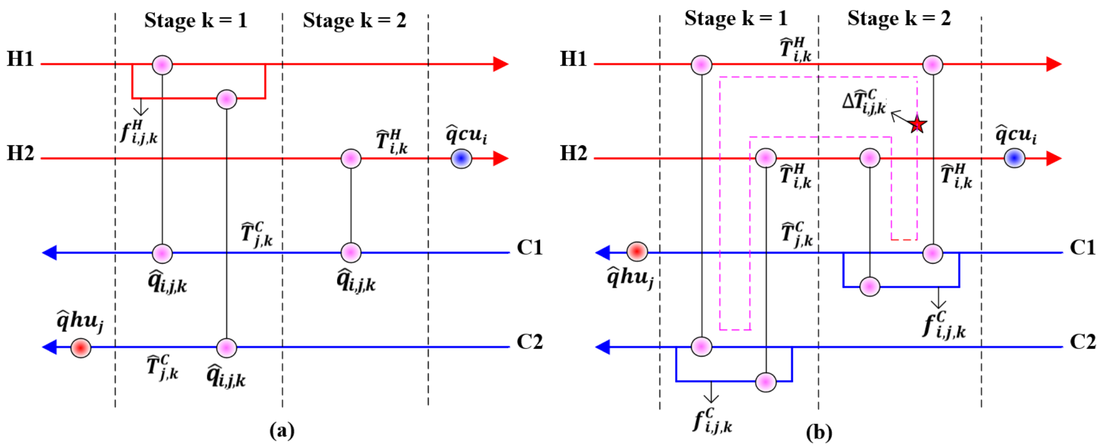

Figure 2. HENs with unique heat loads: (a) MSTR network; (b) Non-MSTR network.

As in previous research, the cost of heat exchanger is given by $C_{i,j,k} = \hat{a}\,\hat{z}_{i,j,k} + \hat{b}\,A^{\hat{c}}_{i,j,k}$. Since the integers ($\hat{z}_{i,j,k}$) are fixed parameters in this problem, the objective function can be reduced to minimizing the sum of the area costs ($\hat{b}\,A^{\hat{c}}_{i,j,k}$). Here, the constant $\hat{b}$ is generally independent of exchanger area, and the objective can be set as minimizing the sum of the concave terms ($A^{\hat{c}}_{i,j,k}$). In addition, without loss of generality, we use the Paterson approximation for the logarithmic mean temperature difference (*LMTD*) since it makes the proof of convexity easier. The nonlinear model (*PS1*) is the following:

$$(PS1)\quad Min \left\{ \sum_{\substack{i\in HP\\ Y_{i,k}^{H}=1}} \sum_{\substack{j\in CP\\ Y_{j,k}^{C}=1}} \sum_{\substack{k\in ST\\ \hat{z}_{i,j,k}=1}} A_{i,j,k}^{\hat{c}} + \sum_{\substack{i\in HP\\ Y_{i,k}^{H}=1}} \sum_{\substack{j\in CP\\ Y_{j,k}^{C}=0}} \sum_{\substack{k\in ST\\ \hat{z}_{i,j,k}=1}} A_{i,j,k}^{\hat{c}} + \sum_{\substack{i\in HP\\ Y_{i,k}^{H}=0}} \sum_{\substack{j\in CP\\ Y_{j,k}^{C}=1}} \sum_{\substack{k\in ST\\ \hat{z}_{i,j,k}=1}} A_{i,j,k}^{\hat{c}} \right\} \tag{3}$$

$$\sum_{j\in CP,\hat{z}_{i,j,k}=1} f_{i,j,k}^{H} - Fcp_{i}^{H} = 0 \qquad \forall i\in HP, k\in ST, Y_{i,k}^{H}=1 \tag{4}$$

$$\sum_{i\in HP,\hat{z}_{i,j,k}=1} f_{i,j,k}^{C} - Fcp_{j}^{C} = 0 \qquad \forall j\in CP, k\in ST, Y_{j,k}^{C}=1 \tag{5}$$

$$\hat{q}_{i,j,k} = f_{i,j,k}^{H}\left(\hat{T}_{i,k}^{H} - t_{i,j,k}^{H}\right) \qquad \forall i\in HP, j\in CP, k\in ST, \hat{z}_{i,j,k}=1, Y_{i,k}^{H}=1 \tag{6}$$

$$\hat{q}_{i,j,k} = f_{i,j,k}^{C}\left(t_{i,j,k}^{C} - \hat{T}_{j,k+1}^{C}\right) \qquad \forall i\in HP, j\in CP, k\in ST, \hat{z}_{i,j,k}=1, Y_{j,k}^{C}=1 \tag{7}$$

$$\Delta t_{i,j,k}^{C} = t_{i,j,k}^{H} - \hat{T}_{j,k+1}^{C} \qquad \forall i\in HP, j\in CP, k\in ST, \hat{z}_{i,j,k}=1, Y_{i,k}^{H}=1 \tag{8}$$

$$\Delta t_{i,j,k}^{H} = \hat{T}_{i,k}^{H} - t_{i,j,k}^{C} \qquad \forall i\in HP, j\in CP, k\in ST, \hat{z}_{i,j,k}=1, Y_{j,k}^{C}=1 \tag{9}$$

$$\hat{q}_{i,j,k}\,\hat{U}_{i,j}^{-1}\,A_{i,j,k}^{-1} - \frac{2}{3}\sqrt{\Delta t_{i,j,k}^{C}\,\Delta t_{i,j,k}^{H}} - \frac{\Delta t_{i,j,k}^{C}}{6} - \frac{\Delta t_{i,j,k}^{H}}{6} \le 0$$
$$\forall i\in HP, j\in CP, k\in ST, \hat{z}_{i,j,k}=1, Y_{i,k}^{H}=1, Y_{j,k}^{C}=1 \tag{10}$$

$$\hat{q}_{i,j,k}\,\hat{U}_{i,j}^{-1}\,A_{i,j,k}^{-1} - \frac{2}{3}\sqrt{\left(\hat{T}_{i,k}^{H} - \hat{T}_{j,k}^{C}\right)\Delta t_{i,j,k}^{C}} - \frac{\hat{T}_{i,k}^{H} - \hat{T}_{j,k}^{C}}{6} - \frac{\Delta t_{i,j,k}^{C}}{6} \le 0$$
$$\forall i\in HP, j\in CP, k\in ST, \hat{z}_{i,j,k}=1, Y_{i,k}^{H}=1, Y_{j,k}^{C}=0 \tag{11}$$

$$\hat{q}_{i,j,k}\,\hat{U}_{i,j}^{-1}\,A_{i,j,k}^{-1} - \frac{2}{3}\sqrt{\left(\hat{T}_{i,k+1}^{H} - \hat{T}_{j,k+1}^{C}\right)\Delta t_{i,j,k}^{H}} - \frac{\hat{T}_{i,k+1}^{H} - \hat{T}_{j,k+1}^{C}}{6} - \frac{\Delta t_{i,j,k}^{H}}{6} \le 0$$
$$\forall i\in HP, j\in CP, k\in ST, \hat{z}_{i,j,k}=1, Y_{i,k}^{H}=0, Y_{j,k}^{C}=1 \tag{12}$$

$$\Delta t_{i,j,k}^{C} \ge EMAT_{Min} \qquad \forall i\in HP, j\in CP, k\in ST, \hat{z}_{i,j,k}=1, Y_{i,k}^{H}=1 \tag{13}$$

$$\Delta t_{i,j,k}^{H} \ge EMAT_{Min} \qquad \forall i\in HP, j\in CP, k\in ST, \hat{z}_{i,j,k}=1, Y_{j,k}^{C}=1 \tag{14}$$

In the above model, we define the variables for both the heat capacity flowrates and temperatures of the sub-streams: $f_{i,j,k}^{H}$ and $t_{i,j,k}^{H}$ for hot streams; $f_{i,j,k}^{C}$ and $t_{i,j,k}^{C}$ for cold streams. Note that equations (13) and (14) are needed because the temperatures involved are variables. This model in the current form is a nonconvex problem because the objective function is concave ($\hat{c}$ is usually smaller than one) and bilinear constraints in equations (6) and (7) are both non-convex. The model *PS1* is now reformulated as a convex model shown as follows.

We rewrite equations (6) and (7):

$$t^H_{i,j,k} = \hat{T}^H_{i,k} - \frac{\hat{q}_{i,j,k}}{f^H_{i,j,k}} \qquad \forall i \in HP, j \in CP, k \in ST, \hat{z}_{i,j,k} = 1, Y^H_{i,k} = 1 \tag{15}$$

$$t^C_{i,j,k} = \hat{T}^C_{j,k+1} + \frac{\hat{q}_{i,j,k}}{f^C_{i,j,k}} \qquad \forall i \in HP, j \in CP, k \in ST, \hat{z}_{i,j,k} = 1, Y^C_{j,k} = 1 \tag{16}$$

Substituting $t^H_{i,j,k}$ and $t^C_{i,j,k}$ by their expressions in constraints (15) and (16) and also substituting the areas ($A_{i,j,k}$), we obtain the following problem namely *PS2*.

$$Min \left\{ \begin{aligned} & \sum_{\substack{i\in HP \\ Y^H_{i,k}=1}} \sum_{\substack{j\in CP \\ Y^C_{j,k}=1}} \sum_{\substack{k\in ST \\ \hat{z}_{i,j,k}=1}} \left(\frac{\hat{q}_{i,j,k}\, \hat{U}^{-1}_{i,j}}{\left[\begin{aligned} & \frac{2}{3}\sqrt{\left(\hat{T}^H_{i,k} - \hat{T}^C_{j,k+1} - \frac{\hat{q}_{i,j,k}}{f^H_{i,j,k}}\right)\left(\hat{T}^H_{i,k} - \hat{T}^C_{j,k+1} - \frac{\hat{q}_{i,j,k}}{f^C_{i,j,k}}\right)} \\ & + \frac{1}{6}\left(\hat{T}^H_{i,k} - \hat{T}^C_{j,k+1} - \frac{\hat{q}_{i,j,k}}{f^H_{i,j,k}}\right) + \frac{1}{6}\left(\hat{T}^H_{i,k} - \hat{T}^C_{j,k+1} - \frac{\hat{q}_{i,j,k}}{f^C_{i,j,k}}\right) \end{aligned} \right]} \right)^{\hat{c}} \\ & + \sum_{\substack{i\in HP \\ Y^H_{i,k}=1}} \sum_{\substack{j\in CP \\ Y^C_{j,k}=0}} \sum_{\substack{k\in ST \\ \hat{z}_{i,j,k}=1}} \left(\frac{\hat{q}_{i,j,k}\, \hat{U}^{-1}_{i,j}}{\left[\begin{aligned} & \frac{2}{3}\sqrt{\left(\hat{T}^H_{i,k} - \hat{T}^C_{j,k}\right)\left(\hat{T}^H_{i,k} - \hat{T}^C_{j,k+1} - \frac{\hat{q}_{i,j,k}}{f^H_{i,j,k}}\right)} \\ & + \frac{1}{6}\left(\hat{T}^H_{i,k} - \hat{T}^C_{j,k}\right) + \frac{1}{6}\left(\hat{T}^H_{i,k} - \hat{T}^C_{j,k+1} - \frac{\hat{q}_{i,j,k}}{f^H_{i,j,k}}\right) \end{aligned} \right]} \right)^{\hat{c}} \\ & + \sum_{\substack{i\in HP \\ Y^H_{i,k}=0}} \sum_{\substack{j\in CP \\ Y^C_{j,k}=1}} \sum_{\substack{k\in ST \\ \hat{z}_{i,j,k}=1}} \left(\frac{\hat{q}_{i,j,k}\, \hat{U}^{-1}_{i,j}}{\left[\begin{aligned} & \frac{2}{3}\sqrt{\left(\hat{T}^H_{i,k+1} - \hat{T}^C_{j,k+1}\right)\left(\hat{T}^H_{i,k} - \hat{T}^C_{j,k+1} - \frac{\hat{q}_{i,j,k}}{f^C_{i,j,k}}\right)} \\ & + \frac{1}{6}\left(\hat{T}^H_{i,k+1} - \hat{T}^C_{j,k+1}\right) + \frac{1}{6}\left(\hat{T}^H_{i,k} - \hat{T}^C_{j,k+1} - \frac{\hat{q}_{i,j,k}}{f^C_{i,j,k}}\right) \end{aligned} \right]} \right)^{\hat{c}} \end{aligned} \right\} \tag{17}$$

$$\sum_{j\in CP, \hat{z}_{i,j,k}=1} f^H_{i,j,k} - Fcp^H_i = 0 \qquad \forall i \in HP, k \in ST, Y^H_{i,k} = 1 \tag{18}$$

$$\sum_{i\in HP, \hat{z}_{i,j,k}=1} f^C_{i,j,k} - Fcp^C_j = 0 \qquad \forall j \in CP, k \in ST, Y^C_{j,k} = 1 \tag{19}$$

$$\hat{q}_{i,j,k} + f_{i,j,k}^{H}\left(\hat{T}_{j,k+1}^{C} - \hat{T}_{i,k}^{H} + EMAT_{Min}\right) \leq 0$$
$$\forall i \in HP, j \in CP, k \in ST, \hat{z}_{i,j,k} = 1, Y_{i,k}^{H} = 1 \tag{20}$$

$$\hat{q}_{i,j,k} + f_{i,j,k}^{C}\left(\hat{T}_{j,k+1}^{C} - \hat{T}_{i,k}^{H} + EMAT_{Min}\right) \leq 0$$
$$\forall i \in HP, j \in CP, k \in ST, \hat{z}_{i,j,k} = 1, Y_{j,k}^{C} = 1 \tag{21}$$

The objective function is a sum of convex terms. Indeed, the terms are the inverse of the *LMTD* function elevated to a constant $\hat{c}$. We recognize that *LMTD* is concave as proven by Mistry and Misener.[27] Even if we use an approximation, this continues to be true. In the Supplemental Material-Part B, we have provided the proof that the objective function of *PS2* is convex. In turn, the system of equations corresponding to the KKT condition of *PS2,* which we solve in the Strategy 3 are presented in the Supplemental Material-Part C. Because the problem is convex, one can just solve this system of equations and obtain the optimum. While it is known that solving these equations directly for large scale systems can exhibit difficulties, we have not observed them in our work.

4. Maximum and Minimum Energy Models

Before performing the Golden Search for a minimal or non-minimal network, it is necessary to obtain the energy bounds E_{Min}^{Niso} and E_{Max}^{Niso}. For non-isothermal mixing, E_{Min}^{Niso} and E_{Max}^{Niso} are in general different from E_{Min}^{Iso} and E_{Max}^{Iso} (isothermal mixing). For this, we develop models namely PE_{Min}^{Niso} and PE_{Max}^{Niso} to obtain E_{Min}^{Niso} and E_{Max}^{Niso} respectively. The formulation of PE_{Min}^{Niso} is the following:

$$PE_{Min}^{Niso} = \min_{\forall (T,Q) \in D_{Synheat}} E \tag{22}$$

$$E = \sum_{j \in CP, \hat{z}hu_j = 1} qhu_j \tag{23}$$

$$\sum_{j \in CP, \hat{z}_{i,j,k} = 1} f_{i,j,k}^{H} - Fcp_i^{H} = 0 \qquad \forall i \in HP, k \in ST, Y_{i,k}^{H} = 1 \tag{24}$$

$$\sum_{i \in HP, \hat{z}_{i,j,k} = 1} f_{i,j,k}^{C} - Fcp_j^{C} = 0 \qquad \forall j \in CP, k \in ST, Y_{j,k}^{C} = 1 \tag{25}$$

$$\Delta t_{i,j,k}^{C} = \left(T_{i,k}^{H} - \frac{q_{i,j.k}}{f_{i,j,k}^{H}} \right) - T_{j,k+1}^{C} \qquad \forall i \in HP, j \in CP, k \in ST, \hat{z}_{i,j,k} = 1, Y_{i,k}^{H} = 1 \tag{26}$$

$$\Delta t_{i,j,k}^{H} = T_{i,k}^{H} - \left(T_{j,k+1}^{C} + \frac{q_{i,j.k}}{f_{i,j,k}^{C}} \right) \qquad \forall i \in HP, j \in CP, k \in ST, \hat{z}_{i,j,k} = 1, Y_{j,k}^{C} = 1 \tag{27}$$

$$\Delta t_{i,j,k}^{C} = T_{i,k+1}^{H} - T_{j,k+1}^{C} \qquad \forall i \in HP, j \in CP, k \in ST, \hat{z}_{i,j,k} = 1, Y_{i,k}^{H} = 0 \tag{28}$$

$$\Delta t_{i,j,k}^{H} = T_{i,k}^{H} - T_{j,k}^{C} \qquad \forall i \in HP, j \in CP, k \in ST, \hat{z}_{i,j,k} = 1, Y_{j,k}^{C} = 0 \tag{29}$$

$$\Delta thu_j = Thu^{out} - T_{j,1}^{C} \qquad \forall j \in CP, \hat{z}hu_j = 1 \tag{30}$$

$$\Delta tcu_i = T_{i,K}^{H} - Tcu^{out} \qquad \forall i \in HP, \hat{z}cu_i = 1 \tag{31}$$

$$\Delta t_{i,j,k}^{C} \geq EMAT_{Min} \qquad \forall i \in HP, j \in CP, k \in ST, \hat{z}_{i,j,k} = 1 \tag{32}$$

$$\Delta t_{i,j,k}^{H} \geq EMAT_{Min} \qquad \forall i \in HP, j \in CP, k \in ST, \hat{z}_{i,j,k} = 1 \tag{33}$$

$$\Delta thu_j \geq EMAT_{Min} \qquad \forall j \in CP, \hat{z}hu_j = 1 \tag{34}$$

$$\Delta tcu_i \geq EMAT_{Min} \qquad \forall i \in HP, \hat{z}cu_i = 1 \tag{35}$$

It should be noted that the variables qhu_j do not participate/present explicitly in any other equations in this model. However, they are implicit in *DSynheat* (Synheat).

The formulation of PE_{Max}^{Niso} presents the same constraints of PE_{Min}^{Niso}(equations (24)-(35)), but the objective function is:

$$PE_{Max}^{Niso} = \max_{\forall (T,Q) \in D_{Synheat}} E \tag{36}$$

The above two models are both non-convex problems and can be solved using a global solver. However, we solve a system of equations (named Sy_E) and we propose two algorithms, namely PBE_{Min} and PBE_{Max}, to obtain the minimum and maximum energy bounds, respectively. The system of equations Sy_E is composed of the constraints of PE_{Min}^{Niso} (equations (24)-(35)) associated to the substitution of the variable E in equation (23) by a fixed parameter ($\hat{E}$):

$$\hat{E} = \sum_{j \in CP, \hat{z}hu_j = 1} qhu_j \tag{37}$$

The algorithm PBE_{Min} is composed of the following steps:

1. Start from $E_{Min}^{Lo} = E_{Min}^{User}$.
2. Run PE_{Min} to obtain E_{Min}^{Iso} and set $E_{Min}^{Up} = E_{Min}^{Iso}$.
3. If $\frac{E_{Min}^{Up} - E_{Min}^{Lo}}{E_{Min}^{Up}} < \hat{\varepsilon}$, go to Step 6. Otherwise, go to next step.
4. Solve Sy_E for $\hat{E} = E_{Min}^{Lo}$. If feasible, $E_{Min}^{Up} = E_{Min}^{Lo}$ and go to Step 6. Otherwise, go to next step.
5. Solve Sy_E for $\hat{E} = \frac{E_{Min}^{Up} + E_{Min}^{Lo}}{2}$. If feasible, $E_{Min}^{Up} = \frac{E_{Min}^{Up} + E_{Min}^{Lo}}{2}$. Otherwise, $E_{Min}^{Lo} = \frac{E_{Min}^{Up} + E_{Min}^{Lo}}{2}$. Then, go to Step 3.
6. $E_{Min}^{Niso} = E_{Min}^{Up}$ and stop.

The algorithm PBE_{Max} is composed of the following steps:

1. Start from $E_{Max}^{Up} = E_{Max}^{User}$.
2. Run PE_{Max} to obtain E_{Max}^{Iso} and set $E_{Max}^{Lo} = E_{Max}^{Iso}$.
3. If $\frac{E_{Max}^{Up} - E_{Max}^{Lo}}{E_{Max}^{Up}} < \hat{\varepsilon}$, go to Step 6. Otherwise, go to next step.
4. Solve Sy_E for $\hat{E} = E_{Max}^{Up}$. If feasible, $E_{Max}^{Lo} = E_{Max}^{Up}$ and go to Step 6. Otherwise, go to next step.
5. Solve Sy_E for $\hat{E} = \frac{E_{Max}^{Up} + E_{Max}^{Lo}}{2}$. If feasible, $E_{Max}^{Lo} = \frac{E_{Max}^{Up} + E_{Max}^{Lo}}{2}$. Otherwise, $E_{Min}^{Up} = \frac{E_{Max}^{Up} + E_{Max}^{Lo}}{2}$. Then, go to Step 3.
6. $E_{Max}^{Niso} = E_{Max}^{Lo}$ and stop.

5. Revisitation of Binding EMAT Location Models

In our part II, two models, namely *PLOC1* and *PLOC,* are used to find the EMAT-binding location of the energy loop of non-MSTR. We now present a new version of *PLOC1* namely *PLOC1S* that includes equations (24)-(35) and the following ones:

$$\beta \geq EMAT_{Min} \tag{38}$$

$$\beta \leq \Delta t^{H}_{i,j,k} \qquad \forall i \in HP, j \in CP, k \in ST, \hat{z}_{i,j,k} = 1 \tag{39}$$

$$\beta \leq \Delta t^{C}_{i,j,k} \qquad \forall i \in HP, j \in CP, k \in ST, \hat{z}_{i,j,k} = 1 \tag{40}$$

$$\beta \leq \Delta thu_j \qquad \forall j \in CP, \hat{z}hu_j = 1 \tag{41}$$

$$\beta \leq \Delta tcu_i \qquad \forall i \in HP, \hat{z}cu_i = 1 \tag{42}$$

$$\left(\Delta t^{H}_{i,j,k} - \beta\right) + \left(1 - y^{H}_{i,j,k}\right) \Gamma_{i,j} \geq 0 \qquad \forall i \in HP, j \in CP, k \in ST, \hat{z}_{i,j,k} = 1 \tag{43}$$

$$\left(\Delta t^{H}_{i,j,k} - \beta\right) + \left(y^{H}_{i,j,k} - 1\right) \Gamma_{i,j} \leq 0 \qquad \forall i \in HP, j \in CP, k \in ST, \hat{z}_{i,j,k} = 1 \tag{44}$$

$$\left(\Delta t^{C}_{i,j,k} - \beta\right) + \left(1 - y^{C}_{i,j,k}\right) \Gamma_{i,j} \geq 0 \qquad \forall i \in HP, j \in CP, k \in ST, \hat{z}_{i,j,k} = 1 \tag{45}$$

$$\left(\Delta t^{C}_{i,j,k} - \beta\right) + \left(y^{C}_{i,j,k} - 1\right) \Gamma_{i,j} \leq 0 \qquad \forall i \in HP, j \in CP, k \in ST, \hat{z}_{i,j,k} = 1 \tag{46}$$

$$\left(\Delta thu_j - \beta\right) + \left(1 - yhu_j\right) \Gamma_j \geq 0 \qquad \forall j \in CP, \hat{z}hu_j = 1 \tag{47}$$

$$\left(\Delta thu_j - \beta\right) + \left(yhu_j - 1\right) \Gamma_j \leq 0 \qquad \forall j \in CP, \hat{z}hu_j = 1 \tag{48}$$

$$(\Delta tcu_i - \beta) + (1 - ycu_i)\, \Gamma_i \geq 0 \qquad \forall i \in HP, \hat{z}cu_i = 1 \tag{49}$$

$$(\Delta tcu_i - \beta) + (ycu_i - 1)\, \Gamma_i \leq 0 \qquad \forall i \in HP, \hat{z}cu_i = 1 \tag{50}$$

$$\sum_{i \in HP} \sum_{j \in CP} \sum_{k \in ST, \hat{z}_{i,j,k}=1,} \left(y^{H}_{i,j,k} + y^{C}_{i,j,k}\right) + \sum_{\hat{z}hu_j = 1} yhu_j + \sum_{\hat{z}cu_i = 1} ycu_i \geq 1 \tag{51}$$

Once *PLOC1S* is solved, the value of energy consumption (E^{*}), heat loads of heat exchangers ($q^{*}_{i,j,k}$, qhu^{*}_j and qcu^{*}_i) as well as the values of $y^{H*}_{i,j,k}$, $y^{C*}_{i,j,k}$, yhu^{*}_j and ycu^{*}_i that represent the potential EMAT-binding location are obtained.

In turn, model *PLOC* is revised as the one namely *PLOCS* that is the system of equations including equations (24)-(35) and the following ones:

$$\sum_{j \in CP, \hat{z}hu_j = 1} qhu_j = E^* \tag{52}$$

$$q_{i,j,k} = q^*_{i,j,k} - \hat{\Delta} \qquad \forall i \in HP, j \in CP, k \in ST, \hat{z}_{i,j,k} = 1, y^{H*}_{i,j,k} = 1 \vee y^{C*}_{i,j,k} = 1 \tag{53}$$

$$qhu_j = qhu^*_j - \hat{\Delta} \qquad \forall j \in CP, \hat{z}hu_j = 1, yhu^*_j = 1 \tag{54}$$

$$qcu_i = qcu^*_i - \hat{\Delta} \qquad \forall i \in HP, \hat{z}cu_i = 1, ycu^*_i = 1 \tag{55}$$

If *PLOCS* is feasible, the energy loop, represented by the binary parameters $y^{H*}_{i,j,k}$, $y^{C*}_{i,j,k}$, yhu^*_j and ycu^*_i, is found. Otherwise, the location does not belong to the energy loop. Then, we exclude this location to find another potential one by running *PLOC1S* again. In a word, *PLOC1S* and *PLOCS* are run recursively until the former is infeasible.

6. Binding EMAT Bounds Models

For non-minimal network with fixed energy consumption, it is necessary to obtain the lower and upper bounds ($\hat{E}MAT_{Min}$ and $\hat{E}MAT_{Max}$) of the binding EMAT with the fixed location. For this purpose, we develop two models namely $PEMAT^{Niso}_{Min}$ and $PEMAT^{Niso}_{Max}$ shown as follows.

The formulation of $PEMAT^{Niso}_{Min}$ includes equations (24)-(35) and the following ones:

$$PEMAT^{Niso}_{Min} = \min_{\forall (T,Q) \in D_{Synheat}} EMAT \tag{56}$$

$$\sum_{j \in CP, \hat{z}hu_j} qhu_j = \hat{E} \tag{57}$$

$$\left(\Delta t^{H}_{i,j,k} - EMAT\right) + \left(1 - y^{H*}_{i,j,k}\right) \Gamma_{i,j} \geq 0 \qquad \forall i \in HP, j \in CP, k \in ST, \hat{z}_{i,j,k} = 1 \tag{58}$$

$$\left(\Delta t_{i,j,k}^{H}-EMAT\right)+\left(y_{i,j,k}^{H*}-1\right)\Gamma_{i,j}\leq 0 \qquad \forall i\in HP, j\in CP, k\in ST, \hat{z}_{i,j,k}=1 \tag{59}$$

$$\left(\Delta t_{i,j,k}^{C}-EMAT\right)+\left(1-y_{i,j,k}^{C*}\right)\Gamma_{i,j}\geq 0 \qquad \forall i\in HP, j\in CP, k\in ST, \hat{z}_{i,j,k}=1 \tag{60}$$

$$\left(\Delta t_{i,j,k}^{C}-EMAT\right)+\left(y_{i,j,k}^{C*}-1\right)\Gamma_{i,j}\leq 0 \qquad \forall i\in HP, j\in CP, k\in ST, \hat{z}_{i,j,k}=1 \tag{61}$$

$$\left(\Delta thu_{j}-EMAT\right)+\left(1-yhu_{j}^{*}\right)\Gamma_{j}\geq 0 \qquad \forall j\in CP, \hat{z}hu_{j}=1 \tag{62}$$

$$\left(\Delta thu_{j}-EMAT\right)+\left(yhu_{j}^{*}-1\right)\Gamma_{j}\leq 0 \qquad \forall j\in CP, \hat{z}hu_{j}=1 \tag{63}$$

$$(\Delta tcu_{i}-EMAT)+(1-ycu_{i}^{*})\,\Gamma_{i}\geq 0 \qquad \forall i\in HP, \hat{z}cu_{i}=1 \tag{64}$$

$$(\Delta tcu_{i}-EMAT)+(ycu_{i}^{*}-1)\,\Gamma_{i}\leq 0 \qquad \forall i\in HP, \hat{z}cu_{i}=1 \tag{65}$$

The formulation of $PEMAT_{Max}^{Niso}$ is composed of the same constraints of $PEMAT_{Min}^{Niso}$ associated to the following objective function:

$$PEMAT_{Max}^{Niso}=\max_{\forall(T,Q)\in D_{Synheat}} EMAT \tag{66}$$

The above nonlinear models $PEMAT_{Min}^{Niso}$ and $PEMAT_{Max}^{Niso}$ can be solved using a global solver. Instead, we solve the following system of equations namely Sy_{EMAT} and develop two algorithms namely $PBEMAT_{Min}$ and $PBEMAT_{Max}$ to obtain the minimum and maximum bounds of the binding EMAT respectively. The system of equations Sy_{EMAT} corresponds to constraints of $PEMAT_{Min}^{Niso}$ but equations (58)-(65) are replaced by the following ones:

$$\left(\Delta t_{i,j,k}^{H}-\hat{E}MAT\right)+\left(1-y_{i,j,k}^{H*}\right)\Gamma_{i,j}\geq 0 \qquad \forall i\in HP, j\in CP, k\in ST, \hat{z}_{i,j,k}=1 \tag{67}$$

$$\left(\Delta t_{i,j,k}^{H}-\hat{E}MAT\right)+\left(y_{i,j,k}^{H*}-1\right)\Gamma_{i,j}\leq 0 \qquad \forall i\in HP, j\in CP, k\in ST, \hat{z}_{i,j,k}=1 \tag{68}$$

$$\left(\Delta t_{i,j,k}^{C}-\hat{E}MAT\right)+\left(1-y_{i,j,k}^{C*}\right)\Gamma_{i,j}\geq 0 \qquad \forall i\in HP, j\in CP, k\in ST, \hat{z}_{i,j,k}=1 \tag{69}$$

$$\left(\Delta t_{i,j,k}^{C}-\hat{E}MAT\right)+\left(y_{i,j,k}^{C*}-1\right)\Gamma_{i,j}\leq 0 \qquad \forall i\in HP, j\in CP, k\in ST, \hat{z}_{i,j,k}=1 \tag{70}$$

$$\left(\Delta thu_{j}-\hat{E}MAT\right)+\left(1-yhu_{j}^{*}\right)\Gamma_{j}\geq 0 \qquad \forall j\in CP, \hat{z}hu_{j}=1 \tag{71}$$

$$\left(\Delta thu_{j}-\hat{E}MAT\right)+\left(yhu_{j}^{*}-1\right)\Gamma_{j}\leq 0 \qquad \forall j\in CP, \hat{z}hu_{j}=1 \tag{72}$$

$$\left(\Delta tcu_i - \hat{E}MAT\right) + (1 - ycu_i^*)\,\Gamma_i \geq 0 \qquad \forall i \in HP, \hat{z}cu_i = 1 \tag{73}$$

$$\left(\Delta tcu_i - \hat{E}MAT\right) + (ycu_i^* - 1)\,\Gamma_i \leq 0 \qquad \forall i \in HP, \hat{z}cu_i = 1 \tag{74}$$

The algorithm $PBEMAT_{Min}$ includes the following steps:

1. Start from $\hat{E}MAT_{Min}^{Lo} = EMAT_{Min}$.
2. Run $PEMAT_{Min}^{Niso}$ to obtain $\hat{E}MAT_{Min}^{Up}$.
3. If $\frac{\hat{E}MAT_{Min}^{Up} - \hat{E}MAT_{Min}^{Lo}}{\hat{E}MAT_{Min}^{Up}} < \hat{\varepsilon}$, go to Step 6. Otherwise, go to next step.
4. Solve Sy_{EMAT} for $\hat{E}MAT = \hat{E}MAT_{Min}^{Lo}$. If feasible, $\hat{E}MAT_{Min}^{Up} = \hat{E}MAT_{Min}^{Lo}$ and go to Step 6. Otherwise, go to next step.
5. Solve Sy_{EMAT} for $\hat{E}MAT = \frac{\hat{E}MAT_{Min}^{Up} + \hat{E}MAT_{Min}^{Lo}}{2}$. If feasible, $\hat{E}MAT_{Min}^{Up} = \frac{\hat{E}MAT_{Min}^{Up} + \hat{E}MAT_{Min}^{Lo}}{2}$. Otherwise, $\hat{E}MAT_{Min}^{Lo} = \frac{\hat{E}MAT_{Min}^{Up} + \hat{E}MAT_{Min}^{Lo}}{2}$. Then, go to Step 3.
6. $\hat{E}MAT_{Min} = \hat{E}MAT_{Min}^{Up}$ and stop.

The algorithm $PBEMAT_{Max}$ includes the following steps:

1. Start from $\hat{E}MAT_{Max}^{Up} = HRAT_{Max}^{User}$.
2. Run $PEMAT_{Max}^{Niso}$ to obtain $\hat{E}MAT_{Max}^{Lo}$.
3. If $\frac{\hat{E}MAT_{Max}^{Up} - \hat{E}MAT_{Max}^{Lo}}{\hat{E}MAT_{Max}^{Up}} < \hat{\varepsilon}$, go to Step 6. Otherwise, go to next step.
4. Solve Sy_{EMAT} for $\hat{E}MAT = \hat{E}MAT_{Max}^{Lo}$. If feasible, $\hat{E}MAT_{Max}^{Up} = \hat{E}MAT_{Max}^{Lo}$ and go to Step 6. Otherwise, go to next step.
5. Solve Sy_{EMAT} for $\hat{E}MAT = \frac{\hat{E}MAT_{Max}^{Up} + \hat{E}MAT_{Max}^{Lo}}{2}$. If feasible, $\hat{E}MAT_{Max}^{Up} = \frac{\hat{E}MAT_{Max}^{Up} + \hat{E}MAT_{Max}^{Lo}}{2}$. Otherwise, $\hat{E}MAT_{Max}^{Lo} = \frac{\hat{E}MAT_{Max}^{Up} + \hat{E}MAT_{Max}^{Lo}}{2}$. Then, go to Step 3.
6. $\hat{E}MAT_{Max} = \hat{E}MAT_{Max}^{Up}$ and stop.

7. Global Optimal Search Algorithm

The algorithm steps are the following.

1. The Synheat model (see Appendix A of Part I) is run without the area costs to minimize the number of heat exchangers (N_{min}) with the given energy bounds $\hat{E}_{Min}^{User}$ and $\hat{E}_{Max}^{User}$. This step is exactly same as the one in parts I and II and the models involved were presented there. Also, set $N = N_{min}$ and start by giving a large value to the incumbent *TAC* namely $UBTAC = +\infty$. Go to next step.
2. For current *N*, run one of the following two options.
   - Option 1: Run *PLB* to enumerate a structure.
   - Option 2: Run *PSTR* to enumerate a structure.
3. If the chosen strategy is not Strategy 1, go to next step. Otherwise, solve the resulting NLP using a global solver (e.g. BARON) for the considered structure to obtain the cost TAC_{STR} and then go to Step 5.
4. For the considered structure, obtain the values of $Y_{i,k}^{H}$ and $Y_{j,k}^{C}$ to ascertain if there is stream split in it.
   a. If there is no split, use the appropriate Golden Search-based algorithms from part I and II to obtain the cost TAC_{STR}.
   b. If there exist split, incorporate the split flows optimization steps outlined above to obtain the cost TAC_{STR} using Strategy 2 or Strategy 3 when obtaining the *TAC* for each value of the energy consumption and the binding *EMAT*.

   Then, go to next step.
5. Update *UBTAC*: If $TAC_{STR} < UBTAC$, $UBTAC = TAC_{STR}$. Go to next step.

6. Exclude previously found structures by running one of the following options.

   - Option 1: run *PLBR* to enumerate another structure. If it is feasible and $RTAC \leq UBTAC$, go to Step 3. Otherwise, if infeasible or if feasible but $RTAC > UBTAC$, go to Step 7.

   - Option 2: run *PSTRR* to enumerate another structure. If feasible, go to Step 3. Otherwise, go to Step 7.

7. If $N > NH+NC+NHU+NCU$, output *UBTAC* and stop. Otherwise, increase the total number of heat exchangers by $N=N+1$ and go to Step 2.

8. Results

Sixteen examples of different sizes that are examples 1-16 used in our parts I and II, as well as three additional new examples are solved. All examples are implemented in GAMS (version 23.7)[41] on a PC machine (i7 3.6 GHz, 8 GB RAM). The solution results are presented in Table 1 that also includes the solution results from our part II for comparison purposes. The total number of the structures enumerated is same as the one in our part II, and hence only TACs and solution time are listed and compared. The solution times for Strategies 1, 2 and 3, proposed in this work, are presented in Table 2.

Table 1 shows the TACs of Examples 2, 5, 6, 16, 17, 18 and 19 are reduced by 1.2 - 8.6 % when considering non-isothermal mixing. Meanwhile, the TACs of examples 1 and 3 are same as the ones in our part II, because there are no stream splits in the optimal solutions. The TACs of Examples 4, 7, 8, 9, 10, 11, 12, 13, 14, 15 decrease slightly (≤1.0 %), showing that the optimal solutions of isothermal and non-isothermal mixing are very closed in these problems. Table 1 also shows that in Examples 1-7 our Option

1 (using *PLB,* smart enumeration using a lower bound) is faster than Option 2 (*PSTR*; exhaustive enumeration). This is mainly due to the fact that Examples 1-7 are not large-scale problems and the lower bound (*PLB*) model in Option 1 can update the lower bounds effectively. On the contrary, for Examples 8-16, Option 2 (*PSTR*) is faster, since these problems are large-scale cases. This shows that when size increases, the solution time becomes larger and the option using the lower bound (*PLB*) model is not viable, unless this smart search is paralelized. Note that we have tried to use different number of intervals to construct the lower bound (*PLB*) model, for instance 2, 5, 8, 10, 20, 30, 40, 50, 60, 70, 80 etc. Then, we picke the number of intervals that renders the minimum solution time. Future work will explore new ways to decrease the solution time. All the solution results are compared with the ones in our Part II or the best literature solutions in the Supplemental Material-Part D.

Regarding strategies, Table 2 indicates that in Examples 1-4 our Strategy 1 using global solver BARON is faster than Strategies 2 and 3. This illustrates BARON could globally and effectively solve the resulting NLP (see the Supplemental Material-Part A) for HEN when the structures are fixed. In Examples 5-16, however, Strategy 1 is slower than Strategies 2 and 3, exhibiting that our Golden Search is better than BARON in these medium- and large-scale problems. Table 2 also shows that Strategy 3 is faster than Strategy 2, demonstrating the applicability of the proposed Lagrange Multiplier method using KKT condition for solving the convex NLM (*PS2*).

Table 1. Solution comparison of Examples 1 – 19

Example	Solutions in part II				Solutions in this work (Part III)			
	PLB		*PSTR*		*PLB*		*PSTR*	
	TAC ($/yr)	Time (s)	TAC ($/yr)	Time (s)	TAC ($/yr)	Time (s)	TAC ($/yr)	Time (s)
1	154,910.6	90.0	154,910.6	168.9	154,910.6	239.1	154,910.6	398.2
2	360,037.2	36.5	360,037.2	162.3	355,701.5	139.5	355,701.5	512.1
3	715,962.9	69.1	715,962.9	196.2	715,962.9	129.2	715,962.9	306.5
4	80,959.6	15.2	80,959.6	369.2	80,847.7	63.2	80,847.7	539.6
5	1,758,381.0	125.6	1,758,381.0	598.2	1,731,819.6	226.8	1,731,819.6	972.5
6	632,360.7	122.3	632,360.7	398.5	624,569.1	239.3	624,569.1	681.3
7	177,261.3	652.3	177,261.3	1932.5	176,097.1	922.7	176,097.1	2833.5
8	-	>360,000	64,015.0	31,502.8	-	>360,000	64015.0	48,335.9
9	-	>360,000	109,078.4	25,659.3	-	>360,000	109,078.4	39,218.8
10	-	>360,000	43,329.2	31,235.8	-	>360,000	43,314.0	53,625.7
11	-	>360,000	3,441,663.0	55,689.3	-	>360,000	3,424,958.8	79,336.5
12	-	>360,000	139,398.1	69,623.8	-	>360,000	139,387.0	82,559.3
13	-	>360,000	6,674,677.0	80,715.9	-	>360,000	6,654,330.1	109,336.8
14	-	>360,000	1,501,004.0	89,625.9	-	>360,000	1,498,935.1	112,758.3
15	-	>360,000	1,414,857.0	100,568.8	-	>360,000	1,407,203.3	183,682.1
16	-	>360,000	1,912,763.0	183,286.5	-	>360,000	1,840,936.2	332,693.6
17	52,430.9	16.8	52,430.9	30.2	48,663.3	56.5	48,663.3	79.3
18	100,770.2	95.9	100,770.2	256.1	95,661.1	199.3	95,661.1	332.5
19	140,367.1	369.8	140,367.1	692.3	128,236.7	589.2	128,236.7	962.5

Table 2. Solution times (s) of strategy 1 - 3

Example	Option 1 (*PLB*)			Option 2 (*PSTR*)		
	Strategy 1	Strategy 2	Strategy 3	Strategy 1	Strategy 2	Strategy 3
1	239.1	380.5	312.6	398.2	502.7	462.6
2	139.5	305.6	236.7	512.1	711.5	620.3
3	129.2	291.3	212.5	306.5	511.3	409.8
4	63.2	101.3	85.3	539.6	737.2	655.2
5	521.6	303.9	226.8	1321.2	1135.6	972.5
6	532.8	318.2	239.3	825.3	765.2	681.3
7	2391.5	1235.9	922.7	3952.8	3361.7	2833.5
8	>360,000	>360,000	>360,000	68,332.5	52,661.7	48,335.9
9	>360,000	>360,000	>360,000	56,335.6	43,205.3	39,218.8
10	>360,000	>360,000	>360,000	68,329.8	59,337.6	53,625.7
11	>360,000	>360,000	>360,000	>360,000	83,329.6	79,336.5
12	>360,000	>360,000	>360,000	>360,000	90,625.8	82,559.3
13	>360,000	>360,000	>360,000	>360,000	113,552.9	109,336.8
14	>360,000	>360,000	>360,000	>360,000	136,621.2	112,758.3
15	>360,000	>360,000	>360,000	>360,000	212,335.6	183,682.1
16	>360,000	>360,000	>360,000	>360,000	379,652.8	332,693.6
17	56.5	72.2	63.5	79.3	95.8	86.2
18	199.3	239.2	212.7	332.5	452.5	401.9
19	792.5	682.5	589.2	1569.1	1322.8	962.5

For illustrating purposes, we present the network designs of Example 2 in Figure 3. It includes the flowsheets of HENs with isothermal and non-isothermal mixing for the optimal structure. From this figure, we find the TAC decreases from 380,338 to 355,700 \$/yr. This is mainly because the total hot utility demand (energy consumption) reduces when allowing non-isothermal mixing (833.9 vs. 676.0 kW). Figure 4 presents the optimal HEN with isothermal mixing assumption from our part II. Comparing Figure 3b and Figure 4, we find both the hot utility demand and area decrease, resulting in 1.2 % saving in TAC. In a word, it is necessary to consider non-isothermal mixing since it has some impact on the trade-offs between the operational and capital costs for HEN synthesis. The network designs of Examples 1-19 are shown in the Supplemental Material-Part D.

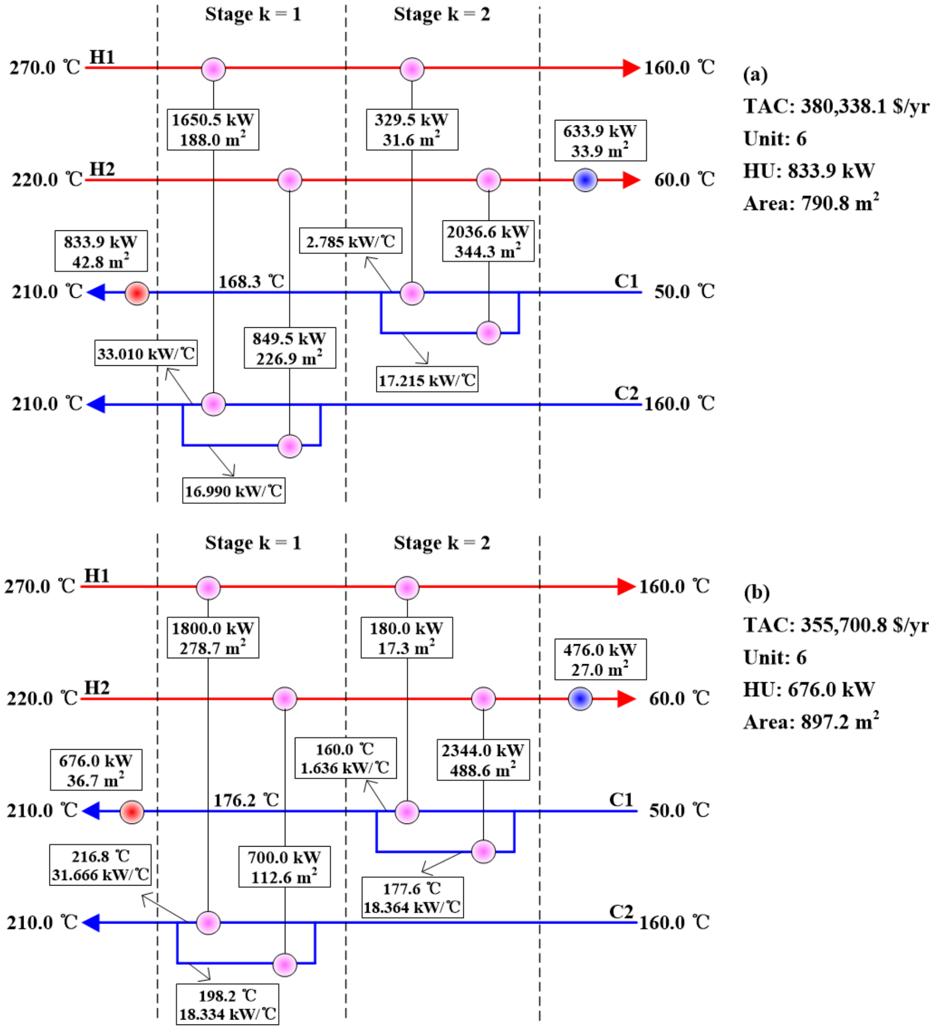

Figure 3. The flowsheets for the optimal structure of example 2: (a) HEN with isothermal mixing; (b) HEN with non-isothermal mixing.

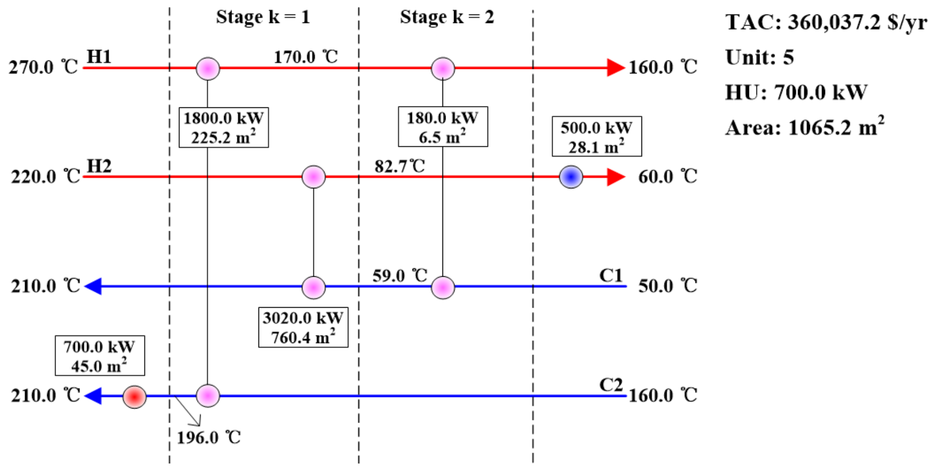

Figure 4. The flowsheets of optimal HEN with isothermal mixing for example 2.

9. Conclusions

In this work, we point out that the heat loads of heat exchangers and the stream temperatures at stages are fixed, either when fixing energy consumption for minimal networks or when fixing energy consumption and the binding EMAT for non-minimal networks. For such two types of HENs, the nonlinear model minimizing the area cost of heat exchangers is proved to be a convex optimization problem that we globally solve using the KKT condition of Lagrange Multiplier method. Meanwhile, we modify the mathematical models proposed in our part I and II to include the constraints for non-isothermal mixing, and develop algorithms to obtain the bounds of energy consumption and the binding EMAT. Based on these, a new Global Optimum Search Algorithm is developed to obtain the globally optimal solutions for minimal and non-minimal HENs with non-isothermal mixing.

The example tests indicate that the TACs can be decreased when considering non-isothermal mixing for HENs. The solution comparisons verify the applicability of the proposed models and algorithms. As we pointed out in the text, one of our strategies are entirely based on mathematical programming-free procedures, with the exception of the candidates enumeration. This enumeration is done using mixed integer linear models, but can also be performed using algorithms based on graph theory and this will be studied in further. New ways/methodologies will be developed to reduce the solution time, especially for large-scale cases. Another further work is to integrate the detailed design of heat exchangers into HEN synthesis.

Acknowledgements

The financial supports of this research are funded by the Project of National Natural Science Foundation of China (NO. 22008210 & 21822809 & 21978256), China Postdoctoral Science Foundation (No. 2019TQ0275 & 2020M671723), the Foundation of State Key Laboratory of High-efficiency Utilization of Coal and Green Chemical Engineering (Grant No.2018-K23). André L. H. Costa thanks the National Council for Scientific and Technological Development (CNPq) for the research productivity fellowship (Process 310390/2019-2) and the financial support of the Prociência Program (UERJ). Miguel J. Bagajewicz would like to thank the Rio de Janeiro State University for its scholarship of Visiting Researcher - PAPD Program.

Notation

Sets

HP	Set of hot process streams indexed by *i*
CP	Set of cold process streams indexed by *j*

ST Set of stages indexed by k

Parameters

N_{min} Minimum number of units

NH Number of hot process streams

NC Number of cold process streams

NHU Number of hot utilities

NCU Number of cold utilities

$Y_{i,k}^{H}$ Binary parameter representing if hot stream i is split or not at stage k

$Y_{j,k}^{C}$ Binary parameter representing if cold stream j is split or not at stage k

$\hat{z}_{i,j,k}$ Binary parameter representing if the exchanger (i, j, k) exists or not

$\hat{z}hu_j$ Binary parameter representing if the heater of cold stream j exists not

$\hat{z}cu_i$ Binary parameter representing if the cooler of hot stream i exists or not

$\hat{q}_{i,j,k}$ Heat load of heat exchanger (i, j, k) for a MSTR or non-MSTR HENs with fixed energy consumption and the binding EMAT

$\hat{q}hu_j$ Heat load of heater (j) for a MSTR or non-MSTR HENs with fixed energy consumption and the binding EMAT

$\hat{q}cu_i$ Heat load of cooler (i) for a MSTR or non-MSTR HENs with fixed energy consumption and the binding EMAT

$\hat{E}$ Fixed energy consumption of hot utility

$\hat{T}_{i,k}^{H}$ Temperature of stream i at stage k upon mixing

$\hat{T}_{j,k}^{C}$ Temperatures of stream j at stage k upon mixing

$\hat{a}$ Fixed installation cost for heat exchanger

$\hat{b}$ Area cost coefficient for heat exchanger

$\hat{c}$ Exponent index for heat exchanger area cost

Fcp_i^{H} Heat capacity folwrate of hot process stream i

$T_{IN,i}$ Inlet temperature of hot process stream i

$T_{OUT,i}$ Outlet temperature of hot process stream i

Fcp_j^{C} Heat capacity folwrate of cold process stream j

$T_{IN,j}$ Inlet temperature of cold process stream j

$T_{OUT,j}$ Outlet temperature of cold process stream *j*

$\hat{\Omega}_i$ Heat content of hot process stream *i*

$\hat{\Omega}_j$ Heat content of cold process stream *j*

$\hat{U}_{i,j}$ Overall heat transfer coefficient for exchanger between stream *i* and *j*

$\hat{U}hu_j$ Overall heat transfer coefficient for the heater of cold streams *j*

$\hat{U}cu_i$ Overall heat transfer coefficient for the cooler of hot streams *i*

$\Gamma_{i,j}$ Upper bound of temperature difference for exchanger bteween streams *i* and *j*

Γ_j Upper bound of temperature difference for the heater of stream *j*

Γ_i Upper bound of temperature difference for the cooler of stream *i*

Thu^{in} Inlet temperature of hot utility

Thu^{out} Outlet temperature of hot utility

Tcu^{in} Inlet temperature of cold utility

Tcu^{out} Outlet temperature of cold utility

$\hat{\varepsilon}$ A small number

$y^{H*}_{i,j,k}$ 1 if the binding EMAT is located at the hot end of heat exchanger (*i*, *j*, *k*) after running model *PLOC1S*

$y^{C*}_{i,j,k}$ 1 if the binding EMAT is located at the cold end of heat exchanger (*i*, *j*, *k*) after running model *PLOC1S*

yhu^*_j 1 if the binding EMAT is located at the cold end of heater (*j*) after running model *PLOC1S*

ycu^*_i 1 if the binding EMAT is located at the hot end of cooler (*i*) after running model *PLOC1S*

E^* Energy consumption obtained by running model *PLOC1S*

$q^*_{i,j,k}$ Heat load of heat exchanger (*i*, *j*, *k*) obtained by running model *PLOC1S*

qhu^*_j Heat load of heater (*j*) obtained by running model *PLOC1S*

qcu^*_i Heat load of cooler (*i*) obtained by running model *PLOC1S*

Binary variables

$z_{i,j,k}$ 1 if the exchanger between streams *i* and *j* at stage *k* exists.

zhu_j 1 if the heater of cold process strean *j* exists.

zcu_i	1 if the cooler of hot process stream *i* exists.
$y_{i,j,k}^H$	1 if the temperature difference at the hot end of exchanger (*i*, *j*, *k*) is the smallest
$y_{i,j,k}^C$	1 if the temperature difference at the cold end of exchanger (*i*, *j*, *k*) is the smallest
yhu_j	1 if the temperature difference at the cold end of heater (*j*) is the smallest
ycu_i	1 if the temperature difference at the hot end of cooler (*i*) is the smallest

Continuous variables

T	Temperature of hot and cold stream at stages in Synheat model
Q	Heat loads of heat exchangers in Synheat model
$q_{i,j,k}$	Heat load of the exchanger between process streams *i* and *j* at stage *k*.
qhu_j	Heat load of the heater for cold process stream *j*.
qcu_i	Heat load of the cooler for hot process stream *i*.
$T_{i,k}^H$	Hot stream *i* temperature at stage *k* upon mixing
$T_{j,k}^C$	Cold stream *j* temperature at stage *k* upon mixing
$f_{i,j,k}^H$	Heat capacity flowrate of the split stream *i* exchanging heat with stream *j* at stage *k*
$f_{i,j,k}^C$	Heat capacity flowrate of the split stream *j* exchanging heat with stream *i* at stage *k*
$t_{i,j,k}^H$	Temperature of the split stream *i* exchanging heat with stream *j* at stage *k*
$t_{i,j,k}^C$	Temperature of the split stream *j* exchanging heat with stream *i* at stage *k*
$\Delta t_{i,j,k}^H$	Temperature difference at the hot end of heat exchanger (*i*, *j*, *k*)
$\Delta t_{i,j,k}^C$	Temperature difference at the cold end of heat exchanger (*i*, *j*, *k*)
Δthu_j	Temperature difference at the cold end of heater *j*
Δtcu_i	Temperature difference at the hot end of cooler *i*
β	Smallest temperature difference for HEN with fixed structure
$A_{i,j,k}$	Area of heat exchanger (*i*, *j*, *k*)
$LMTD$	Logarithmic mean temperature difference
TAC_{STR}	Total annualized cost for a HEN with fixed structure
E_{Min}^{Iso}	Minimum energy for HEN structure with isothermal mixing
E_{Min}^{Niso}	Minimum energy for HEN structure with non-isothermal mixing
E_{Min}^{Lo}	Lower bound of the minimum energy for HEN with fixed structure
E_{Min}^{Up}	Upper bound of the minimum energy for HEN with fixed structure

E_{Max}^{Iso} Maximum energy for HEN structure with isothermal mixing

E_{Max}^{Niso} Maximum energy for HEN structure with non-isothermal mixing

E_{Max}^{Lo} Lower bound of the maximum energy for HEN with fixed structure

E_{Max}^{Up} Upper bound of the maximum energy for HEN with fixed structure

$\hat{E}MAT_{Min}$ Lower bound of the binding EMAT for HEN with fixed structure

$\hat{E}MAT_{Max}$ Upper bound of the binding EMAT for HEN with fixed structure

Model acronym list

$D_{Synheat}$	Synheat model
PSTR	Problem rendering any viable structure of matches and candidates
PSTRR	Problem to enumerate different structures
PLB	Lower bound model rendering any viable structure of matches and candidates
PLBR	Problem containing problem *PLB* and the exclusion constraint
PS1	Non-convex model minimizing area cost for a MSTR and non-MSTR HEN with fixed energy consumption and binding EMAT
PS2	Convex model minimizing area cost for a MSTR and non-MSTR HEN with fixed energy consumption and binding EMAT
PE_{Min}^{Niso}	Problem targeting the minimum hot utility energy consumption
PE_{Max}^{Niso}	Problem targeting the maximum hot utility energy consumption
Sy_E	System of equations for targeting energy consumption bounds
PBE_{Min}	Algorithm for obtaining the lower bound of energy consumption
PBE_{Max}	Algorithm for obtaining the upper bound of energy consumption
PLOC1S	Problem to find the possible locations of the binding EMAT
PLOCS	Problem to detect if the EMAT-binding location obtained is part of a loop
$PEMAT_{Min}^{Niso}$	Problem targeting the minimum binding EMAT
$PEMAT_{Max}^{Niso}$	Problem targeting the maximum binding EMAT
Sy_{EMAT}	System of equations for targeting the bounds of the binding EMAT
$PBEMAT_{Min}$	Algorithm for obtaining the lower bound of the binding EMAT
$PBEMAT_{Max}$	Algorithm for obtaining the upper bound of the binding EMAT

References

1. Furman KC, Sahinidis NV. A Critical Review and Annotated Bibliography for Heat Exchanger Network Synthesis in the 20th Century. Industrial & Engineering Chemistry Research. 2002;41(10):2335-2370.
2. Morar M, Agachi PS. Review: Important contributions in development and improvement of the heat integration techniques. Computers & Chemical Engineering. 2010;34(8):1171-1179.
3. Klemeš JJ, Kravanja Z. Forty years of Heat Integration: Pinch Analysis (PA) and Mathematical Programming (MP). Current Opinion in Chemical Engineering. 2013;2(4):461-474.
4. Bogataj M, Kravanja Z. An alternative strategy for global optimization of heat exchanger networks. Applied Thermal Engineering. 2012;43:75-90.
5. Beck A, Hofmann R. How to tighten a commonly used MINLP superstructure formulation for simultaneous heat exchanger network synthesis. Computers & Chemical Engineering. 2018;112:48-56.
6. Yuen A. Synthesis of performance-optimal heat exchanger networks using attainable regions. Computers & Chemical Engineering. 2020;142:107043.
7. Huang KF, Karimi IA. Simultaneous synthesis approaches for cost-effective heat exchanger networks. Chemical Engineering Science. 2013;98:231-245.
8. Huang Kf, Karimi IA. Efficient algorithm for simultaneous synthesis of heat exchanger networks. Chemical Engineering Science. 2014;105:53-68.
9. Hong X, Liao Z, Jiang B, Wang J, Yang Y. New transshipment type MINLP model for heat exchanger network synthesis. Chemical Engineering Science. 2017;173:537-559.
10. Gundersen T, Traedal P, Hashemi-Ahmady A. Improved sequential strategy for the synthesis of near-optimal heat exchanger networks. Computers & Chemical Engineering. 1997;21:S59-S64.
11. Nemet A, Isafiade AJ, Klemeš JJ, Kravanja Z. Two-step MILP/MINLP approach for the synthesis of large-scale HENs. Chemical Engineering Science.

2019;197:432-448.

12. Ziyatdinov NN, Emel'yanov II, Chen Q, Grossmann IE. Optimal heat exchanger network synthesis by sequential splitting of process streams. Computers & Chemical Engineering. 2020;142:107042.
13. Ravagnani MASS, Silva AP, Arroyo PA, Constantino AA. Heat exchanger network synthesis and optimisation using genetic algorithm. Applied Thermal Engineering. 2005;25(7):1003-1017.
14. Fieg G, Luo X, Jeżowski J. A monogenetic algorithm for optimal design of large-scale heat exchanger networks. Chemical Engineering and Processing: Process Intensification. 2009;48(11):1506-1516.
15. Aguitoni MC, Pavão LV, Siqueira PH, Jiménez L, Ravagnani MAdSS. Heat exchanger network synthesis using genetic algorithm and differential evolution. Computers & Chemical Engineering. 2018;117:82-96.
16. Peng F, Cui G. Efficient simultaneous synthesis for heat exchanger network with simulated annealing algorithm. Applied Thermal Engineering. 2015;78:136-149.
17. Pavão LV, Costa CBB, Ravagnani MASS, Jiménez L. Large-scale heat exchanger networks synthesis using simulated annealing and the novel rocket fireworks optimization. AIChE J. 2017;63(5):1582-1601.
18. Silva AP, Ravagnani MASS, Biscaia EC, Caballero JA. Optimal heat exchanger network synthesis using particle swarm optimization. Optim Eng. 2010;11(3):459-470.
19. Huo Z, Zhao L, Yin H, Ye J. Simultaneous synthesis of structural constrained heat exchanger networks with and without stream splits. Can J Chem Eng. 2013;91(5):830-842.
20. Pavão LV, Costa CBB, Ravagnani MAdSS. Automated heat exchanger network synthesis by using hybrid natural algorithms and parallel processing. Computers & Chemical Engineering. 2016;94:370-386.
21. Pavão LV, Costa CBB, Ravagnani MASS. An Enhanced Stage-wise Superstructure for Heat Exchanger Networks Synthesis with New Options for Heaters and Coolers Placement. Industrial & Engineering Chemistry Research. 2018;57(7):2560-2573.

22. Rathjens M, Fieg G. A novel hybrid strategy for cost-optimal heat exchanger network synthesis suited for large-scale problems. Applied Thermal Engineering. 2020;167:114771.
23. Floudas CA, Ciric AR, Grossmann IE. Automatic synthesis of optimum heat exchanger network configurations. AIChE J. 1986;32 (2):276-290.
24. Kim SY, Bagajewicz M. Global optimization of heat exchanger networks using a new generalized superstructure. Chemical Engineering Science. 2016;147:30-46.
25. Yee TF, Grossmann IE. Simultaneous optimization models for heat integration. II, heat exchanger network synthesis. Comput Chem Eng. 1990;14(10):1165-1184.
26. Huang KF, Al-mutairi EM, Karimi IA. Heat exchanger network synthesis using a stagewise superstructure with non-isothermal mixing. Chemical Engineering Science. 2012;73:30-43.
27. Mistry M, Misener R. Optimising heat exchanger network synthesis using convexity properties of the logarithmic mean temperature difference. Computers & Chemical Engineering. 2016;94:1-17.
28. Pavão LV, Costa CBB, Ravagnani MASS. A new stage-wise superstructure for heat exchanger network synthesis considering substages, sub-splits and cross flows. Applied Thermal Engineering. 2018;143:719-735.
29. Beck A, Hofmann R. A Novel Approach for Linearization of a MINLP Stage-Wise Superstructure Formulation. Computers & Chemical Engineering. 2018;112:17-26.
30. Nair SK, Karimi IA. Unified Heat Exchanger Network Synthesis via a Stageless Superstructure. Industrial & Engineering Chemistry Research. 2019;58(15):5984-6001.
31. Chang C, Peccini A, Wang Y, Costa ALH, Bagajewicz MJ. Globally optimal synthesis of heat exchanger networks. Part I: Minimal networks. AIChE J. 2020; 66:e16267.
32. Chang C, Liao Z, Costa ALH, Bagajewicz MJ. Globally optimal synthesis of heat exchanger networks. Part II: Non-minimal networks. AIChE J. 2020;66: e16264.
33. Kim SY, Jongsuwat P, Suriyapraphadilok U, Bagajewicz M. Global Optimization of Heat Exchanger Networks. Part 1: Stages/Substages Superstructure. Industrial &

Engineering Chemistry Research. 2017;56(20):5944-5957.

34. Kim SY, Bagajewicz M. Global Optimization of Heat Exchanger Networks. Part 2: Stages/Substages Superstructure with Variable *Cp*. Industrial & Engineering Chemistry Research. 2017;56(20):5958-5969.
35. Xiang Y, Cui G. A novel Random Walk algorithm with Compulsive Evolution for heat exchanger network synthesis. Chemical Engineering Research and Design. 2017;115:1118-1127.
36. Pavão LV, Costa CBB, Ravagnani MASS. Heat Exchanger Network Synthesis without stream splits using parallelized and simplified simulated Annealing and Particle Swarm Optimization. Chemical Engineering Science. 2017;158:96-107.
37. Zhang H, Cui G. Optimal heat exchanger network synthesis based on improved cuckoo search via Lévy flights. Chemical Engineering Research and Design. 2018;134:62-79.
38. Björk K-M, Westerlund T. Global optimization of heat exchanger network synthesis problems with and without the isothermal mixing assumption. Computers & Chemical Engineering. 2002;26(11):1581-1593.
39. Escobar M, Trierweiler JO. Optimal heat exchanger network synthesis: A case study comparison. Applied Thermal Engineering. 2013;51(1):801-826.
40. Faria DC, Kim SY, Bagajewicz MJ. Global Optimization of the Stage-wise Superstructure Model for Heat Exchanger Networks. Industrial & Engineering Chemistry Research. 2015;54(5):1595-1604.
41. Brooke A, Kendrick D, Meeraus A, Raman R. GAMS: A Users Guide. Washington, DC: GAMS Development; 2005.